

Laser optical simulation of diffraction from distorted lattices

B. K. MATHUR, B. K. SAMANTARAY and G. B. MITRA

*Department of Physics,
Indian Institute of Technology, Kharagpur-721302*

A knowledge of intensity distribution in the reciprocal space for scattering from different types of defects is essential for determining the different types of defect parameters. The optical transform method is one of the powerful techniques for studying the intensity distribution due to different defects. Models of atomic configurations at the edge and screw dislocation in f.c.c. and b.c.c. lattices as well as grain boundaries were obtained using the results of computer simulation studies and the masks were prepared by photographic reduction. Optical transforms of the masks were obtained with the help of a Lipson diffractometer fabricated in the laboratory by using a 1 mW spectra physics He-Ne laser as the source. The rotating optical transforms were taken for obtaining the optical analogue of the powder patterns. It has been observed that the intensity at the reciprocal lattice points splits into annular halos or takes the 'figure of eight' shape in some of the cases. The directional dependence of the splitting has been compared with the existing theories. It has also been observed that with the ordering of the dislocations at the grain boundaries, the diffraction pattern resembles that of the single dislocation. Line profiles of rotating optical transforms have been analysed and the informations regarding the nature of the strain distribution because of different types of defects have been obtained.

1 INTRODUCTION

Due to elastic strain around the lattice defects there is a displacement of atoms from their normal lattice sites. Huang (1947), considering a random distribution of defects, each producing a spherically symmetric displacement field $\mathbf{U} = \frac{c\mathbf{Y}}{|\mathbf{Y}|^3}$, has shown that crystals containing such defects would give rise to a diffuse scattering. Wilson (1949, 1950, 1952, 1955), Vassamillet (1959) and others have given theories of diffraction from crystals containing dislocations and have predicted the nature of the modulation of the intensity distribution. These theories have been further developed by several workers and with improved experimental techniques it has now been possible to obtain the relaxation around the defects from the measurement of the intensity distribution (Dederichs 1973). Comparison of these theories with the experimental studies of the diffuse scattering is rather difficult because of the interference of the thermal diffuse scattering (TDS) with the defect diffuse scattering (DDS). Of course at liquid helium

temperatures the TDS can be considered to be small with respect to the DDS. But this may not give the true picture of the relaxation field around the defects at room temperatures because of the temperature dependence of the atomic bondings etc. Hence it would be helpful if a knowledge of the nature of DDS in different systems is obtained by numerical computation or by optical diffraction techniques where the system is represented by a mask having static atoms. For calculating DDS enormous amount of numerical calculations are involved and hence often one has to make many simplifying assumptions. Moreover, as shown by Keating & Goland (1971) series termination effects in such calculation gives rise to serious errors in the form of ripples in the intensity distribution. Because of the above reasons optical transform studies from models containing different defects would be of great use.

In fact optical transform studies have been applied to a variety of problems viz —for solving crystal structures (Lipson & Taylor 1958), for interpreting small angle scattering (Hosemann 1962), for studying diffraction from fibres (Mukhopadhyay & Taylor 1971) etc. Mitra & Bhattacharjee (1974) have applied it for studying diffraction from curved crystals and Samantaray *et al* (1975) have used it for studying DDS from point defects. So far only Willis (1975a, 1975b) has used the optical transform technique for studying diffraction from dislocations. He has considered only the case of a single edge dislocation and has used the isotropic elastic theory for his model. So far no work on the optical diffraction from screw dislocations and dislocation clusters forming the grain boundaries or rotating optical transforms representing the polycrystalline X-ray diffraction pattern have been reported.

Recently a high degree of sophistication has been achieved in the computer simulation studies of lattice defects (Gehlen *et al* 1972, Beeler 1970) thus enabling one to get a more accurate picture of the atomic configuration at the defects. Hence in the present investigation optical diffraction from edge and screw dislocations and grain boundaries have been taken. Rotating optical transforms have also been taken and informations regarding the nature of the strain distribution around these defects has been obtained. The variation of the tail of the intensity profiles in reciprocal space has also been studied.

2. CHOICE OF THE MODELS

As has been mentioned earlier most of the above works are based on the elastic continuum model which does not give an accurate representation of the atomic structure in the defect region. The elastic continuum theory fails in the region around the core of the dislocation where, according to this theory, the stresses become infinite. Hence computer simulation methods are employed for obtaining a more realistic picture. Excellent reviews of such computer calcula-

tions are available in Gehlen *et al* (1972) and Beeley (1970). In the present investigation the models for the masks of the different defects were made by taking the atomic positions at the defect region from the published works on computer simulation studies.

Masks for the f.c.c. edge dislocation were made by taking the results of Cotterill & Doyoma (1964, 1965); and Doyoma & Cotterill (1966a, 1966b). They have assumed that the dislocation lies along a $\langle 112 \rangle$ direction normal to the plane of the paper. They have observed that in marked contrast to the elastic continuum theory the displacements parallel to both the dislocation line and the slip plane were not zero (at some positions they were about 9% of the near neighbour distance). The central portions of the masks of the f.c.c. edge dislocation based on their result has been shown in figure 1b. Similarly the masks for the $[110]$ screw dislocation were made by taking the results from Cotterill & Doyoma (1965). The central portion of the masks has been shown in figure 2b. The core configuration for the b.c.c. edge dislocation with Burgers vector $b = a \langle 100 \rangle$ was taken from the results of Bulough & Perrin (1970). The relevant portion of the mask has been shown in figure 3b.

It is well known that stable twist grain boundaries are formed by a crossed grid of screw dislocations. The corresponding mask has been shown in figure 4b. Masks for the 6° tilt boundary in γ -iron without and with interstitial carbon impurities were made by taking the computer calculation results of Dahl *et al* (1972). The cases for the 6° tilt boundary and the 6° tilt boundary with 3 carbon atoms has been shown in figures 5b and 6b respectively.

3. EXPERIMENTAL

Drawings of the atomic configurations at the defects were made on a white sheet of paper by plotting atomic coordinates obtained from the computer simulated models described earlier. The atomic positions were blackened with Indian ink and photographs were taken with a reduction ratio of 100:1. The number of atoms taken in each model were to the extent that the strain fields of the defects decreases to negligible value. This was around 10^3 atoms. The negatives placed between two optical flats were used as the masks for obtaining the diffraction patterns. An optical diffractometer was constructed with the geometry similar to the well known Lipson diffractometer, but by replacing the conventional Hg source by a 1 mw Spectra Physics He-Ne laser. For simulating the X-ray diffraction patterns from polycrystalline samples, the masks or the film mount were rotated with the direct beam as the axis. The optical diffraction patterns were recorded on 22 DIN-125 ASA films and were processed under identical conditions. The optical diffraction patterns shown in figures 1a-6a correspond to the masks shown in figures 1b-6b respectively.

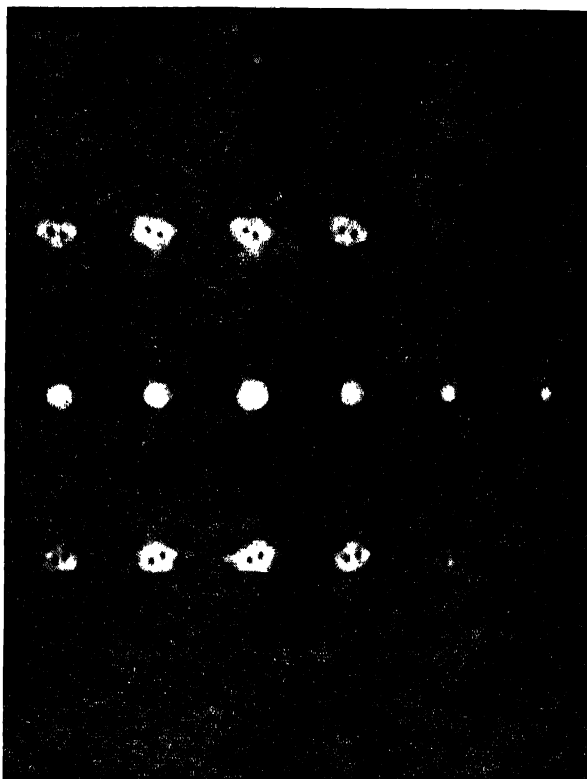


Fig. 1(a) Optical transform of the projection of 6 atomic planes around an edge dislocation in an f.c.c. lattice.

4. RESULTS AND DISCUSSION

(a) *Effect of dislocations on intensity distribution*

The theory of diffraction from a crystal containing a single screw dislocation has been given by Wilson (1949, 1952, 1955) and Frank (1949). Using the Hall (1950) model for displacements Wilson (1950) has calculated the intensity distribution for the edge dislocation. He has observed that the $0k$ reflections are unaffected by the presence of the dislocation where k refers to the direction

normal to the Burgers vector. He has also observed that hk intensity distributions are drawn out into hollow rings and the diameter of the rings are independent of the k but increase with h . Suzuki (1956) and Suzuki & Willis (1956) have shown by considering the diffraction from a model given by the isotropic elastic theory (Rood 1953) that the intensity distribution in the neighbourhood of a hk point is more complex and depends on both h and k . They have observed that the $h0$ reflection is of the shape of figure of eight and the $0k$ reflection is of the shape of a cross. Willis (1957a, 1957b) has taken the optical transforms for

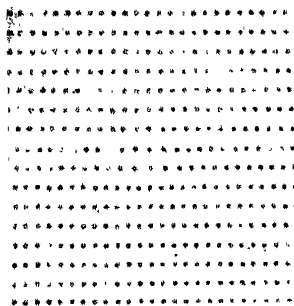


Fig. 1(b) Central portion of the mask. Position of atoms around an edge dislocation in a f.c.c. lattice. It is a projection of 6 atomic planes. The plane of the figure is 112.

both the models and has shown that the optical transforms agree with the theoretical models. In the present case the models were made from the results of the computer simulation studies. It is observed from figure 1a that the hk reflections other than $0k$ type have the shape of a figure of eight. One of the hk reflections has been enlarged and shown in figure 7. In the case of $1k$ reflection a continuous figure of eight pattern is obtained. But for higher h values the spot breaks into several spots which are on a contour of figure of eight shape. However, no change in the $0k$ spots are observed. Thus the $h0$ and hk reflections of the optical transforms of the computer simulated f.c.c. edge dislocations resemble the Suzuki case whereas the $0k$ reflections resembles the Wilson case. In the case of the b.c.c. edge dislocation (figure 3a) it is observed that the different hk reflections have different shapes depending upon their indices. 11 type reflections are found to have the ring type shape whereas the 20 type reflections have the figure of eight shape. The 02 type reflections have a crossed shape similar to the one obtained for the Suzuki case. Thus it is observed that the displacement fields produced because of edge dislocation are quite complex and the different diffraction theories which assume the simple elastic continuum approach do not explain the results fully.

In figure 2a, the optical transform of the atoms in a 111 plane immediately above the slip plane for the screw dislocation in the f.c.c. lattice, it is observed that an annular halo forms around the diffracted spots. The radius of the halo

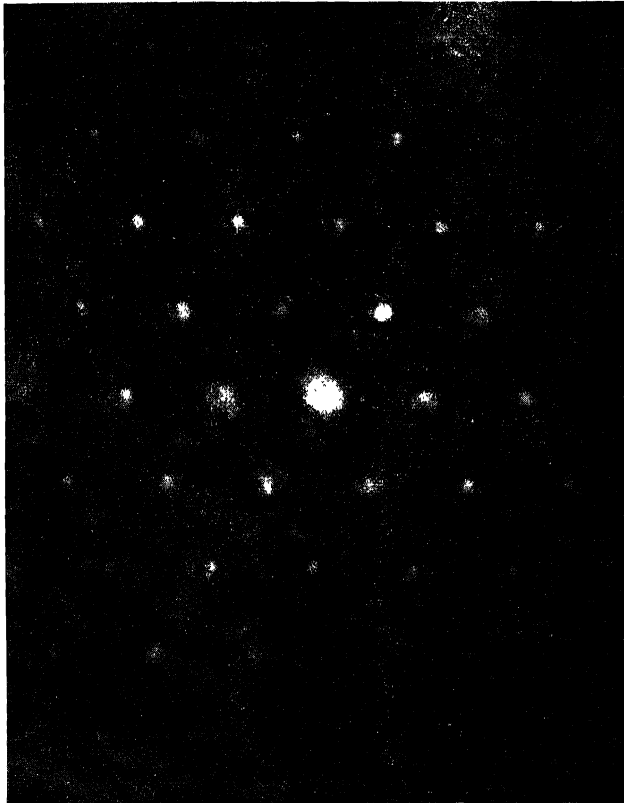


Fig. 2(a). Optical transform of a screw dislocation in an f.c.c. lattice

increases with the increase in the order. However if the entire screw dislocation is considered, possibly the halo will increase in intensity with a corresponding decrease in the intensity at the reciprocal lattice point finally giving rise to the rings as predicted by Wilson (1949). However, the optical method could

not be applied to verify this because of the difficulties in representing in a two dimensional grating the repetition in a third direction of a two dimensional configuration of atoms.

Weak diffuse scattering is also observed in the optical transforms. The diffuse scattering is in the form of streaks joining the reciprocal lattice points. In case of the f.c.c. edge dislocation the streaks are observed to be parallel to the h and k direction whereas in the b.c.c. edge dislocation they are observed to be parallel to the diagonal.

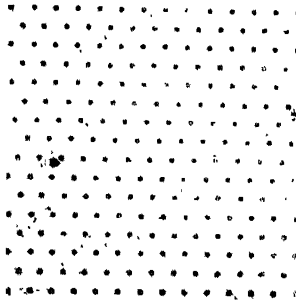


Fig 2(b) Central portion of the mask. Position of the atoms around a screw dislocation in a f.c.c. lattice. The figure shows in a 111 plane immediately above the slip plane.

Optical transform of the grain boundaries have been shown in figures 4a-6a. In the optical transforms of a section of a crossed grid of a screw dislocation giving rise to a twist boundary it is observed that each of the spots splits into a large number of parallel spots. Further strong diffuse streaks are also found to join the reciprocal lattice points. In case of a 6° tilt grain boundary in gamma iron the spots are found to bifurcate. With the addition of a carbon impurity atom at the bad fit region it is observed from the computer simulation experiments that there is an ordering of the dislocations forming the grain boundaries. In the optical transform it is observed that the splitting of the spots gets rounded to resemble the diffraction from edge dislocation. On addition of two more carbon atoms there is further ordering of the dislocations forming the grain boundaries. The optical transform further improves and resembles the diffraction pattern from the edge dislocation. There is a lot of similarity between figures 3a and 6a. Thus it is observed that when there is an ordering of dislocations at the grain boundaries the diffracted intensities resemble that from a single dislocation to a great extent.

(b) *Rotational optical transforms of lattice defects*

The pure X-ray diffraction profiles obtained after correcting for the geometrical broadening is due to various factors like particle size, strain, stacking faults etc. and is therefore a convolution of the line profiles due to each of these.

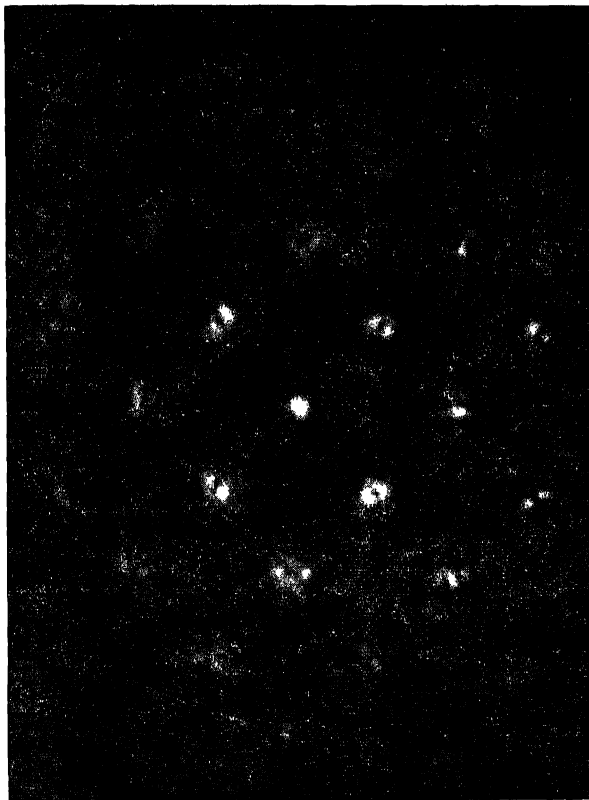


Fig. 3(a) Optical transform from a two layer projection of an edge dislocation in b.c.c. lattice.

In the methods of analysis of the line profile for determining the contributions due to different effects involve assumptions regarding the nature of the individual profiles. In the integral breadth method of analysis, assumptions are made

regarding the nature of the particle size and the strain profiles. The Fourier analysis technique also assumes the strain profile to be of some particular type. Hence in order to determine the validity of the methods applied an idea about the nature of these profiles and the pure diffraction profile is required. Mitra (1963) has discussed the various methods of analysing the nature of the profiles and has shown that the profiles can be any one of Pearson curves.

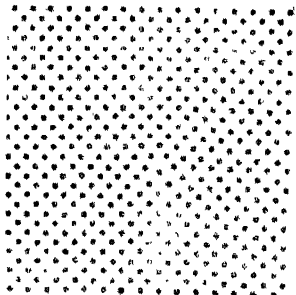


Fig. 3(b). Central portion of the mask. A (010) projection of f.c.c. edge dislocation with Burger vector $a(100)$. There are no displacements in the (010) direction. It is a projection of two layers.

As has been mentioned in the previous sections, the strain fields due to the dislocations and dislocation aggregates spreads the intensity distribution at the reciprocal lattice point. For the powder pattern this would give rise to a broadening of the line profile. Hence in the present case the rotating optical transforms were taken for all the masks mentioned in the previous sections as well as for the undisturbed lattices. One such typical rotating optical transform for the f.c.c. edge dislocation as well as that for the corresponding undeformed lattice have been shown in figures 9 and 8 respectively.

It is clearly seen by comparing the two that there is a broadening of the line profiles in the one containing the dislocations. This broadening being due to the strain fields at the dislocation. Hence an analysis of the corrected line profile would give informations regarding the nature of the strain profile for the dislocations. The analysis for finding out the nature of the strain profile was carried out in the following manner.

It is well known that even if the difference between the two direct distributions is not appreciable, the difference between the corresponding cumulative distributions is much more prominent. This property of the cumulative distributions is made use of in the $N(z)$ test for distinguishing between contro-

symmetric and non-centro-symmetric space groups. Utilizing this characteristic, Mitra (1963) has developed a method for deciding whether a given line profile belongs to the Cauchy or Gauss type.

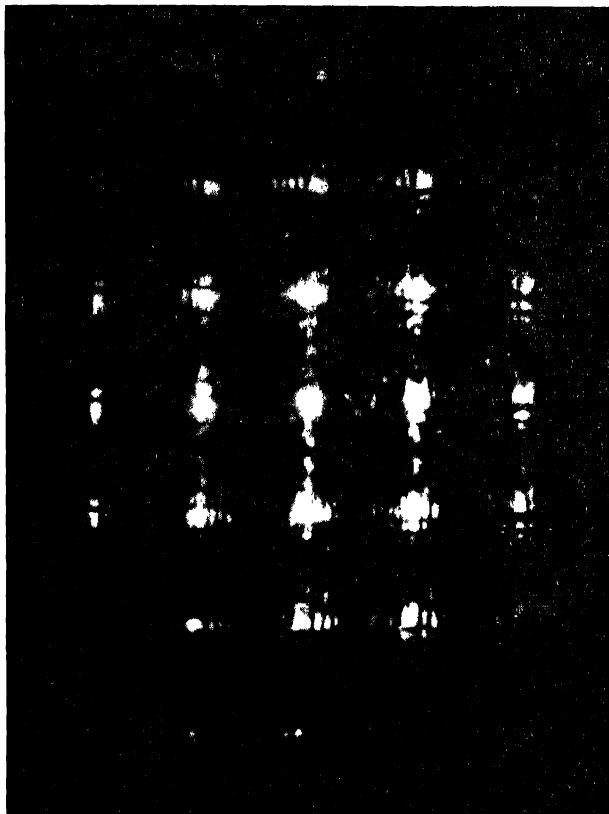


Fig. 4(a) Optical transform of twist boundary formed by crossed grid of screw dislocations.

Suppose that the intensity distribution of the line under study about the Bragg angle θ_0 is given by $I(\theta)$. The angles at which the intensity merges in the background be θ_1 and θ_2 respectively. Since both the Cauchy and Gauss distributions are symmetrical, let $\theta_0 - \theta_1 = \theta_2 - \theta_0 = N$ (say). For the purpose of studying the distribution, let us put $\theta_0 = \theta$ so that the intensity spread is

effectively between $\pm N$. Let σ be the standard deviation of the distribution and let $\frac{\theta - \theta_0}{\sigma} = x$ be the new variable for the angle spread. Let us introduce a scalar c , so that

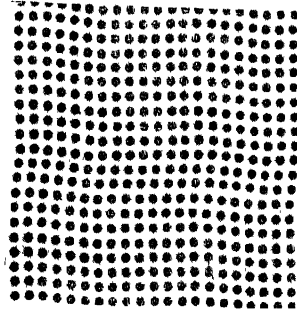


Fig. 4(b) Central portion of the mask. Twist boundary formed by crossed grid of screw dislocations (sectional)

$$c I(\theta) = F(\theta)$$

and

$$\int_{-N/\sigma}^{+N/\sigma} F(x) dx = 1$$

In terms of the new variable x , the distribution has been denoted by $F(x)$. The cumulative distribution has been defined by

$$R(x) = \int_0^x F(x) dx$$

It is easy to show that for the Gaussian distribution,

$$R(x) = \frac{1}{2} \operatorname{erf} \frac{x}{\sqrt{2}}$$

and for Cauchy type,

$$R(x) = \frac{1}{\pi} \tan^{-1} x.$$

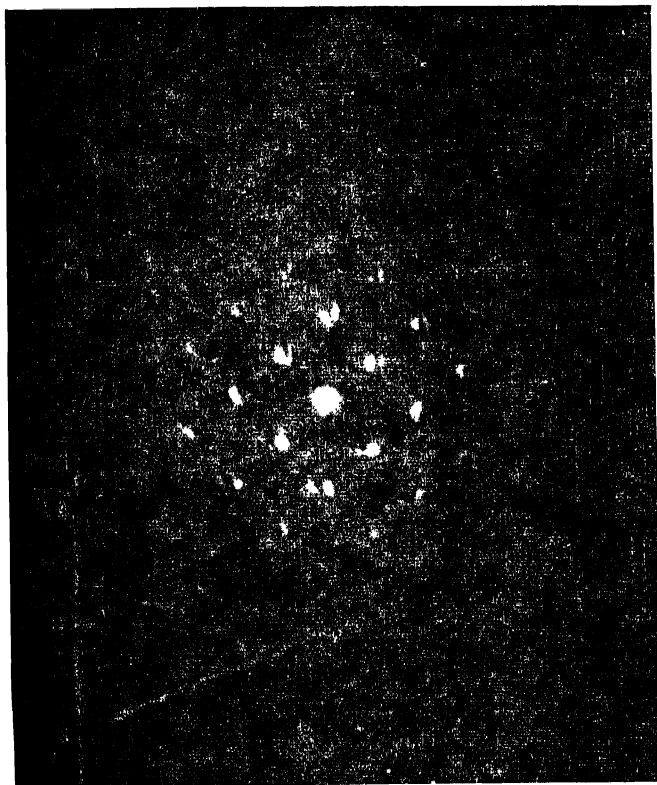


Fig. 5(a) Optical transform of a 6-degree tilt grain boundary in Gamma-iron 100 plane

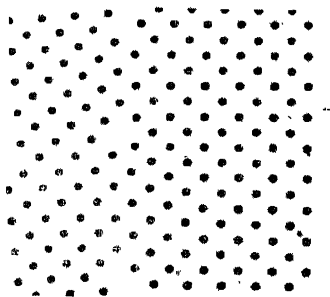


Fig. 5(b) Central portion of the mask.

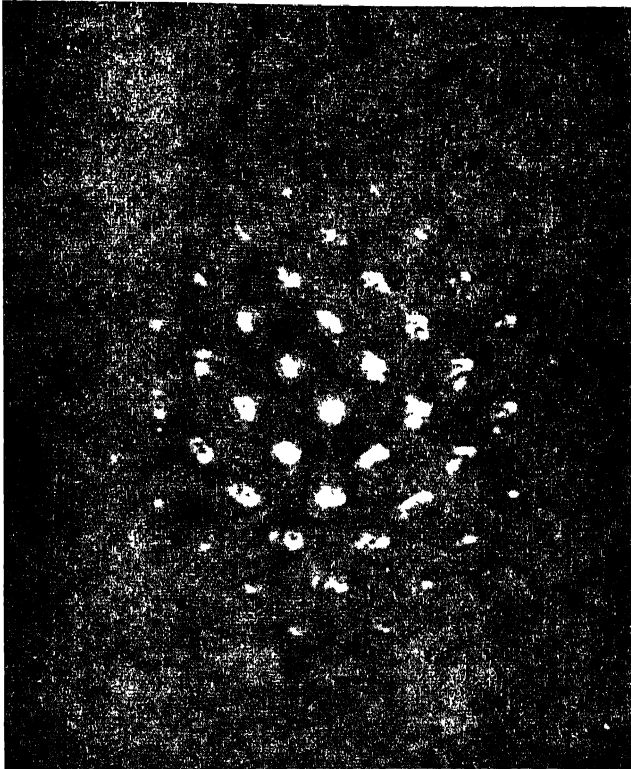


Fig. 6(a) Optical transform of a 6-degree tilt grain boundary with three carbon interstitials in bad fit region

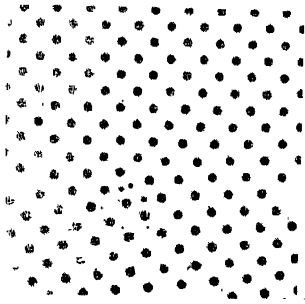


Fig. 6(b) Central region of the mask.



Fig. 7. Figures of 8 obtained in f.c.c. edge dislocation optical transform

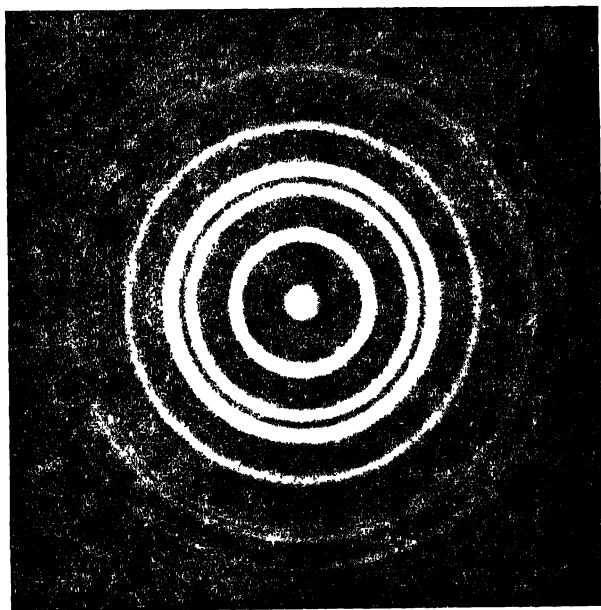


Fig. 8. Rotational optical transform from undistorted lattice,

Another method of determining the nature of the line profile is by finding out the ratio $\beta = \mu_4/\mu_2$ where μ_1 and μ_2 are the fourth and second central moments

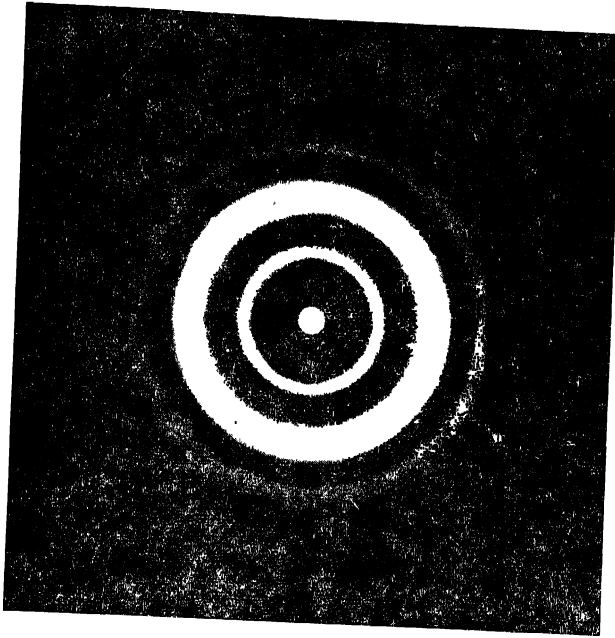


Fig. 9. Rotational optical transform of an f.c.c. lattice of figure 1(b), having one edge dislocation.

respectively. For the cases where the asymmetry of the profiles is negligible, as shown by Pearson & Heartley (1956), we have

for $\beta = 2.5$ to 3.5 —the curve is Gaussian (N)

$\beta = 3.5$ to 5 —the curve is Pearson type IV given by

$$\gamma = \gamma_0 e^{-\nu \tan^{-1} \frac{x}{a}} \left(1 + \frac{x^2}{a^2} \right)^{-m}$$

x between $-\infty$ to $+\infty$

$\beta = 3.5$ to 4 , —the curve belong to Pearson type VII given by

$$\gamma = \gamma_0 \left(1 + \frac{x^2}{a^2} \right)^{-m}$$

It may be mentioned here that Cauchy is a special type of Pearson curve VII with $m = 1$.

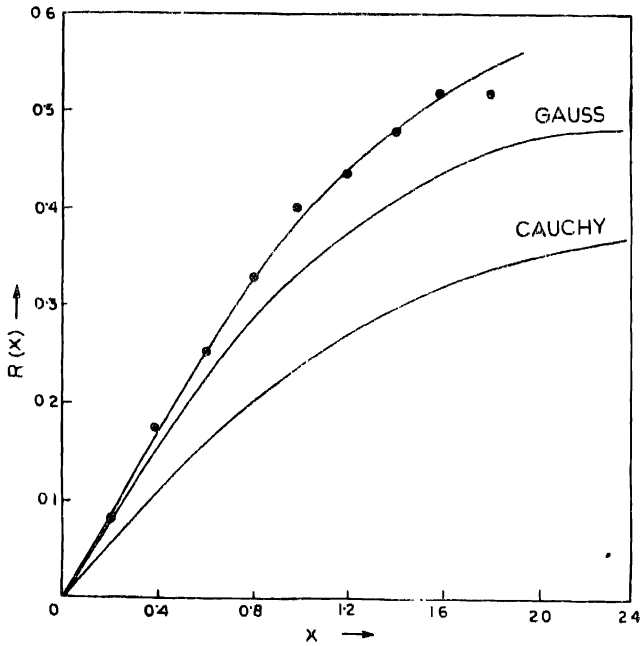


Fig. 10. $R(x)$ test for case of (10) line profile from f.c.c. edge dislocation.

In the present case the values of $R(x)$ of the corrected profile were calculated for various values of x and were plotted along with the theoretical one. One such plot for the case of f.c.c. edge dislocation has been shown in figure 10. It is observed that the experimental points do not fit exactly either the Gauss or the Cauchy curves but lies close to the Gaussian curve. Similar results were also obtained for b.c.c. edge and f.c.c. screw dislocations. This shows that the strain profiles for the dislocations are close to Gaussian. However in case of the Grain boundaries they lie in the middle of the two curves showing that the strain profiles are neither Gaussian nor Cauchy type but are more complex.

The values of $\beta = \mu_1/\mu_2$ for the different cases have been shown in table I. The first three profiles of each case for which measurements were made gave

almost the same value of β . It is observed that for the case of the single dislocations we have Gaussian values whereas for grain boundaries the curve types are different

Table 1. Values of $\beta = \mu_1/\mu_2$ for different profiles

| | β | Curve type |
|------------------|---------|------------|
| f.c.c. edge | 2.6 | N |
| b.c.c. edge | 2.4 | N |
| f.c.c. screw | 2.8 | N |
| Twist boundary | 3.6 | VII |
| 6° tilt boundary | 3.7 | VII |

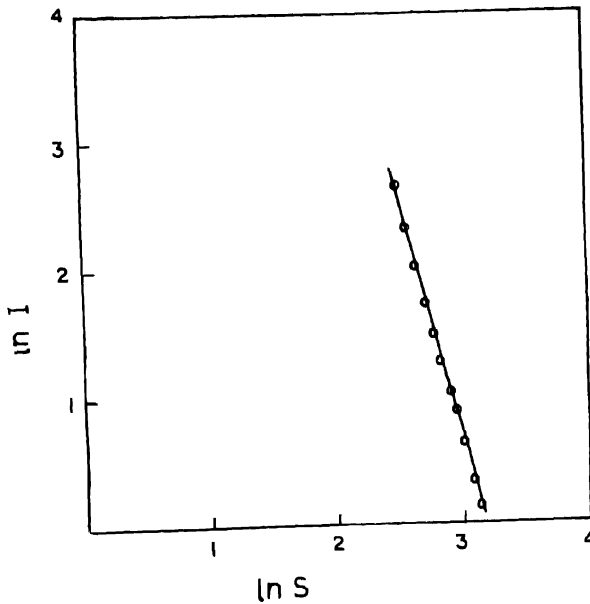


Fig. 11. Double log plot of the variation in the intensity at the tails with the distance from the centre of the (10) profile for the case of the f.c.c. edge dislocation.

(c) *Variation of the intensity at the tails of the profiles*

Because of the $r/|r|^3$ behaviour of the displacement fields the intensity of the Huang diffuse scattering varies as $1/q^2$, where q is the deviation from the reciprocal lattice point. Wilson (1955) has obtained expressions for the falling off of the intensities at the tails of the line profiles and has shown that the tails tend to zero as the inverse cube of the distance from the centre of the profile. Vassamillet (1959) has shown from the numerical computations of the intensity expression that the intensity does not fall as the inverse cube but decreases more rapidly. As has been discussed by Dederichs (1973), since the displacement near the core vary at a rate greater than $1/r^2$, the intensity at the further end of the tails may decrease at a faster rate than the inverse fourth power. Hence in the present investigation a double log plot of the intensity with the distance from the centre of the line was made. The plots were straight lines with slopes between -3.5 and -4.0 . One typical such plot has been shown in figure 11.

REFERENCES

- Beeler Jr. J. R. 1970 *Advances in Material Research*, Vol IV, p. 295, (ed. H. Herman Interscience Publishers, New York).
- Bullough R. & Peirin R. C. T. P. 292, *AERE Report*, Harwell, England (As quoted in Beeler, 1970).
- Cotterill R. M. J. & Doyama H. 1964 *Phys. Letters* **13**, 110.
- Cotterill R. M. J. & Doyama M. 1965 *Phys. Letters* **14**, 79.
- Dohl R. E., Beeler J. R. & Bourgoin R. D. 1972 *Interatomic Potentials and Simulation of Lattice Defects*, p. 582, ed. Gehlen *et al* (Plenum Press, New York).
- Dederichs P. H. 1973 *J. Phys. F.* **3**, 471.
- Doyama M. & Cotterill R. M. J. 1966a *Phys. Rev.* **145**, 465.
- Doyama M. & Cotterill R. M. J. 1966 *Phys. Rev.* **150**, 448.
- Frank F. C. 1949 *Research* **2**, 542.
- Gehlen P. C., Beeler J. R. & Jaffee R. I. 1972 *Interatomic Potentials and Simulation of Lattice Defects* (Plenum Press, New York).
- Hall W. H. 1950 *Ph.D. Thesis* (Birmingham).
- Hosemann R. 1962 *Polymer* **3**, 349.
- Huang K. 1947 *Proc. Roy. Soc.* **A190**, 102.
- Keating D. T. & Goland A. N. 1971 *Acta Cryst.* **A27**, 134.
- Lipson H. & Taylor C. A. 1958 *Fourier Transforms and X-ray Diffraction* (G. Bell & Sons, London).
- Mitra G. B. 1963 *Acta Cryst.* **16**, 429.
- Mitra G. B. & Bhattacharyya S. 1974 *Ind. J. Phys.* **48**, 520.
- Mukhopadhyay U. & Taylor C. A. 1971 *J. Appl. Cryst.* **4**, 20.
- Pearson E. S. & Hartley H. O. 1956 *Biometrical Tables for Statisticians*, Vol 1, p. 210 (Camb. Univ. Press).
- Read W. T. 1953 *Dislocations in Crystals* (McGraw-Hill, New York).
- Samantaray B. K., Mathur B. K. & Gupta R. K. 1975 *Ind. J. Phys.* **49**, 521.

- Suzuki T. 1957 As quoted in Willis 1957b
Suzuki T. & Willis B. T. M. 1956 *Nature*, London, **177**, 712.
Vassamillet L. F. 1959 *Il Nuovo Cimento* **13**, 1133.
Willis B. T. M. 1957a *Proc. Roy. Soc.* **A239**, 181
Willis B. T. M. 1957b *Proc. Roy. Soc.* **A239**, 192
Wilson A. J. C. 1949 *Research*, London **2**, 541
Wilson A. J. C. 1950 *Research*, London **3**, 387
Wilson A. J. C. 1952 *Acta Cryst.* **5**, 318
Wilson A. J. C. 1955 *Il Nuovo Cimento* **1**, 277.